# Structure and electronic properties of step edges in the aluminum oxide film on NiAl(110)

L. Heinke, L. Lichtenstein, G. H. Simon, T. König, M. Heyde,* and H.-J. Freund
*Fritz-Haber-Institut der Max-Planck-Gesellschaft, Faradayweg 4-6, D-14195 Berlin, Germany*
(Received 11 May 2010; revised manuscript received 25 June 2010; published 31 August 2010)

Thin film aluminum oxide has been investigated at step edges of the NiAl(110) substrate by means of low temperature scanning tunneling microscopy and atomic force microscopy. A preference of the step edges for certain orientations and a restructuring of the substrate step edges during the oxidation were shown. The surface unit cell of the oxide film at the step edge is similarly extended as at the antiphase domain boundaries (APDBs), which are oxygen deficient defects with $F^{2+}$-like centers. The local electronic structure and the local work function at the step edges resemble that of the APDBs. Therefore, an oxide film structure at the step edge which is similar to the APDB as well as a carpetlike coverage of the substrate steps is concluded. This means there are $F^{2+}$-like centers at step edges.

DOI: 10.1103/PhysRevB.82.075430 PACS number(s): 68.55.−a, 68.37.Ps, 07.79.Cz, 68.47.Gh

## I. INTRODUCTION

Line defects and step edges influence the chemistry on oxide surfaces significantly. Here we investigate the nature of the step edges on thin film aluminum oxide on the NiAl(110) substrate. Aluminum oxide is one of the most common oxide supports for metals in heterogeneous catalysis,[1] and a detailed investigation is therefore of great interest from more than just a scientific point of view. Due to charging effects, many surface techniques cannot be applied to insulators like aluminum oxide. This limitation can be circumvented by using thin oxide films on metal supports as model systems. In this way, thin film aluminum oxide on NiAl(110) was investigated in numerous studies, see e.g., Refs. 2–6. It was found that defects in the thin film have special properties, which influence the chemistry and physics of the surface significantly. These defects can for example enhance chemical activity or act as nucleation centers of metal nanoparticles.[7,8]

In the aluminum oxide film, linear dislocations between two domains of the same orientations are known as antiphase domain boundaries (APDBs).[9–12] Other frequent structural defects are step edges. In this work we investigate the nature of the step edges in the aluminum oxide by means of atomic force and scanning tunneling microscopy. We determined the local electronic structure and the local work function, which exhibit striking similarities with APDBs. Furthermore, conclusions about the structure at the step edges can be drawn and a restructuring of the substrate surface during oxidation is proven.

## II. EXPERIMENTAL SETUP

The experimental setup consists of a dual-mode low-temperature (5 K) scanning tunneling microscope (STM) and frequency modulation atomic force microscope (FM-AFM), also known as noncontact AFM (NC-AFM) or frequency modulation dynamic force microscope (FM-DFM). In the STM mode the tip height is regulated to gain a fixed tunneling current. In the AFM mode, the tip height is regulated to obtain a constant frequency shift of the tuning fork, to which the tip is attached. Tunneling current and frequency shift can be recorded simultaneously and the feedback can be switched between both modes instantly. This means AFM and STM images of exactly the same position on the surface can be recorded with the same microscopic tip configuration. This constitutes the great advantage of this dual-mode setup. For example, this enables the recording of an AFM picture with a fixed frequency shift and simultaneously it facilitates the analysis of the tunneling current, or vice versa. A detailed description of the instrumentation and of the technique can be found in Refs. 13 and 14. The tip in use is composed of 90% platinum and 10% iridium. The experiments are performed in ultrahigh vacuum, i.e., at a pressure below $10^{-7}$ Pa.

The electronic properties of the sample surface are investigated by means of scanning tunneling spectroscopy (STS).[15] This means the conductance is determined as a function of the bias voltage. This is realized by varying the bias voltage $U_{\mathrm{bias}}$ and regulating the tip-sample distance $z$ to keep the tunneling current $I$ at a fixed value. The $\mathrm{d}z/\mathrm{d}U_{\mathrm{bias}}$ versus $U_{\mathrm{bias}}$ spectrum at constant tunneling current is similar to the $\mathrm{d}I/\mathrm{d}U_{\mathrm{bias}}$ versus $U_{\mathrm{bias}}$ spectrum at constant height.[16] The chosen implementation avoids high field strengths at the elevated voltages of up to 6 V and helps to preserve the tip. The local density of electronic states (LDOS) is contained in the spectra.[16] Spectra taken at positive sample bias can confirm the presence of unoccupied states.

The contact potential difference, which is the difference between the work functions of the tip and of the sample surface, can be locally determined by FM-AFM in the Kelvin probe force spectroscopy mode.[17–21] While the $z$ position is constant, the bias voltage between tip and sample is varied, which modifies the electrostatic contribution in the tip-sample interaction and therefore changes the frequency shift.[22,23] When the electrostatic forces are minimal, i.e., the contact potential between sample and surface is canceled out by the bias voltage, the resonance frequency (and therewith the frequency shift) has its maximum value. The contact potentials were determined by recording the frequency shift versus bias voltage curves and fitting these curves with a quadratic term.[22,24] The same set point of the frequency shift, i.e., the same tip-sample interaction, ensures a very similar tip-sample distance. Due to the integration of both techniques into one sensor, bias spectroscopy (in the STM mode)

 

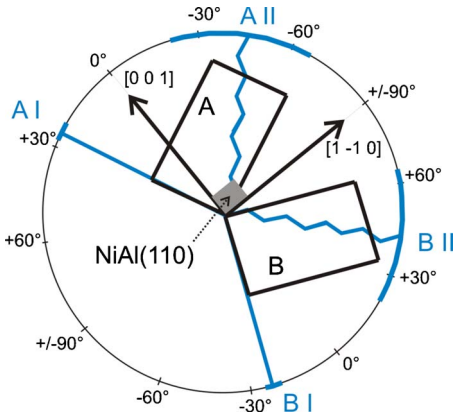


FIG. 1. (Color online) Directions of film and substrate of aluminum oxide on NiAl(110). The rectangular NiAl(110) surface unit cell ($0.29 \times 0.41$ nm$^2$) is shown as gray solid box. The surface unit cells of the two domains (A and B) of the aluminum oxide film are rotated by $\pm 24°$ with respect to [1 −1 0]. They measure 1.06 nm by 1.79 nm enclosing an angle of 88.7°. The angular orientations of the APDB paths are pictured blue. All angles are plotted with respect to [0 0 1] (Ref. 26).

and contact potential measurements (in the AFM mode) can be performed at exactly the same site with the same tip.

## III. STUDIED SYSTEM

The substrate is the NiAl(110) surface, which is densely packed with equal proportions of Ni and Al.[25] Ni and Al are aligned in alternating rows with the Al slightly relaxed outward.[25] Before the oxidation of the surface, the NiAl crystal was $Ar^+$ sputtered and annealed at 1000 °C for more than 5 times to produce a clean and defect-free surface.

Thin film aluminum oxide on NiAl(110) is composed of two oxygen and two aluminum layers.[3] It is prepared in a simple and reliable two step selective oxidation procedure. After dosing $5 \times 10^{-4}$ Pa oxygen for 10 min at 550 K, the sample is heated to 1050 K in vacuum to crystallize the film. The process can be repeated to close open metal patches in the film. The preparation is explained in detail in ref. 2. The film grows in two reflection domains, A and B, which are tilted by $\pm 24°$ with respect to NiAl[1 −1 0] (Fig. 1).[26]

The major structural defects in the film are reflection domain boundaries (A-B), APDBs (A-A or B-B) and step edges in the NiAl substrate surface. While the reflection domain boundaries occur randomly and rarely, APDBs occur regularly, roughly every 8–10 nm to release stress in the perfect oxide film that accumulates due to a small lattice mismatch with the NiAl along the [1 −1 0] direction.

There are multiple types of APDBs, the most common types are straight and zigzagged APDBs.[9,26] At straight APDBs, also called type I, the surface unit cell is extended parallel to the long edge of the oxide unit cell. At zigzagged APDBs (type II) both directions of the unit cell are extended. The orientations of these line defects are shown in Fig. 1. By DFT calculations,[10] the stoichiometry of the film with a straight APDB was determined to be $(NiAl)^{2-}_{substrate}(Al_{19}O_{28}Al_{28}O_{32})^{2+}$. An oxygen deficiency with unoccupied electronic states in the aluminum oxide band gap was determined. These defect states can be referred to as $F^{2+}$ center in the APDB. These $F^{2+}$-like centers were experimentally verified by AFM.[24] The domain boundaries are particularly chemically active. For instance, it was shown by molecular beam methods that nitric oxide decomposes on thin film aluminum oxide preferentially at the APDBs.[7]

## IV. RESULTS AND DISCUSSIONS

### A. Images of the substrate surface and of the oxide film

A typical STM image of the bare NiAl(110) surface before the preparation of the oxide film is shown in Fig. 2(a). The surface is very smooth without defects and impurities. Step edges occur in the smooth surface caused by a small miscut of the crystal surface or by a possibly locally heterogeneous sputtering during preparation. The distance between the steps is roughly some tens of nm. This is consistent with the crystal's miscut angle of less than 0.5°.

The thin film aluminum oxide on NiAl(110) imaged by STM is shown in Figs. 2(b)–2(f). At first glance, it seems that the step edges prefer special orientations, e.g., parallel to the straight APDB or with an angle of approximately 50° to the straight APDB. At most step edges the orientation of the film (domain A or B) is identical on both sides [see Figs. 2(b), 2(c), and 2(e)]. However, the reflection symmetry (A or B) may also change at a step edge [see Fig. 2(d)]. Most step edges have a height of approximately 0.2 nm, which corresponds to one atom layer of the NiAl(110) surface. Step edges with a height of two or more substrate layers occur rarely.

Domain A is much more frequent than B. This might be caused by a better compatibility of domain A with the orientation of the substrate step edges.[27]

### B. Orientation of the step edges

At first glance, substrate step edges seem to prefer special orientations to the APDBs of the oxide film. A detailed analysis of substrate step edge orientations with and without oxide film in comparison to APDB orientations is shown in Fig. 3. The histogram was prepared by vectorizing the line defects, whose orientation was analyzed and plotted. More than 100 STM images have been evaluated. The total length of analyzed APDBs and step edges adds up to about 100 $\mu$m. Before the oxide film is prepared, the step edges on the NiAl(110) are often oriented with an angle of roughly +50° with respect to the [0 0 1] direction [see Fig. 3(a)]. This results from a small miscut of the crystal face.

After oxidation, the APDBs are often oriented along approximately +25° and −25° with respect to [0 0 1] [see Fig. 3(c)], that corresponds to the orientations of the straight APDB in domain A and B, respectively (see Fig. 1). Further orientations of the APDBs result from the zigzagged type, which may adopt various angles, ranging from +20° to +70° and −20° to −70°, respectively.[26]

Step edges in the alumina thin film partly reorient during oxidation. Figure 3(b) shows three preferred orientation peaks of oxide step edges (+25°, +50°, and +70°), which

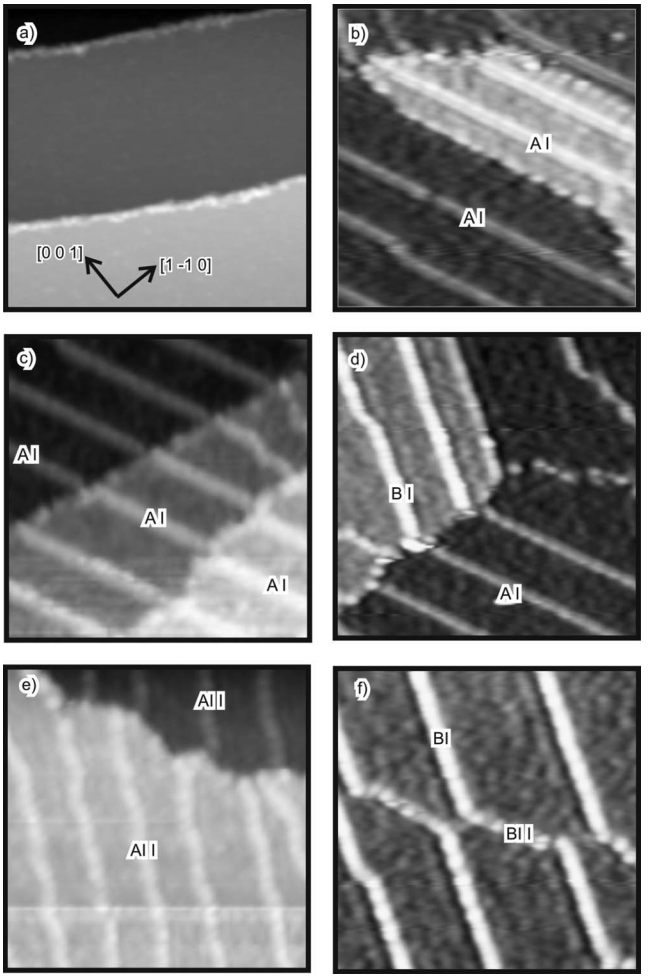


FIG. 2. STM images, $50\times50$ nm$^2$. a) Three different terraces of the NiAl(110) surface. The bias voltage was set to +1 V and the tunneling current was regulated to 100 pA. b)-f) Typical images of thin film aluminum oxide. The APDBs (bright lines) and step edges of the substrate are clearly visible. Some APDBs are labeled (domain A or B, type I or II). Typical features of the film at the step edges are shown: b) The step edges are parallel orientated to the APDB. c) The orientation of the domain and the APDB are continued on the next terraces. d) The domain changes its orientation (A-B) at the step edges. e) APDB of type AII. f) APDB of type BI and BII. The bias voltage in pictures b-f) was set to +3 V and the tunneling current was regulated to 100 pA. The [1 −1 0] and [0 0 1] directions of the substrate indicated in figure a) are common to all images.

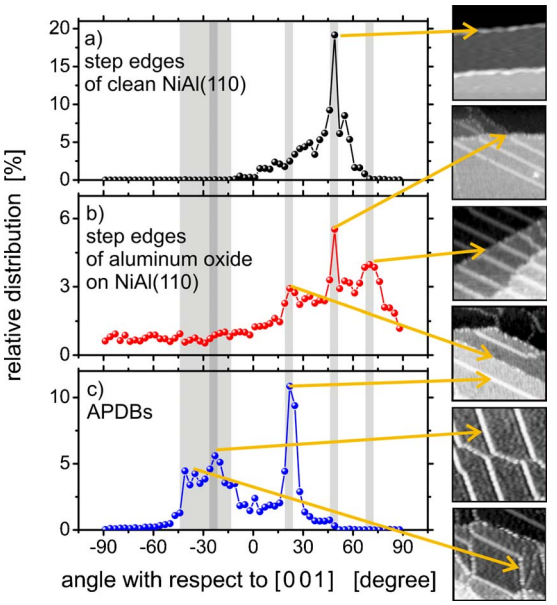


FIG. 3. (Color online) Histogram of the orientation of the substrate step edges before oxide film preparation (a), with oxide film (b) and of the APDB (c). The angles are plotted with respect to the [0 0 1] direction of the substrate (see Fig. 1). Intervals with a size of 3° are summarized in one point. On the right hand side, STM images ($50\times50$ nm$^2$; $U_{\mathrm{bias}}=3$ V, and $I=100$ pA) with a typical step edge or APDB are pictured.

differ, the step edge orientations in the clean substrate surface. The +50° angle is governed by the substrate, indicating that the oxide film covers the metal steps readily. However, the orientations of 25° and 70° rarely occur in the substrate surface before oxidation. During oxidation the substrate steps rearrange to form energetically more favorable directions, which are connected with the oxide film. For instance, steps along 25° are parallel to straight APDBs of domain A. The origin of the 70° orientation might be the macroscopic direction of the substrate step edges, which is given by the crystal's miscut. The film changes the step edges' orientation only locally. So, steps edges along 25° have to be balanced, resulting in a formation of steps with an inclination of more than 50° (e.g., 70°). Note that reorientation of the step edges during oxidation is associated with a rise of the total length of the step edges. The initially straight step edges expand and make curved segments in various directions. So, in addition to the most frequent orientations of the steps (25°, 50°, and 70°), other directions occur that cannot be attributed to characteristic angles neither in the metal nor in the film.

A restructuring of the NiAl substrate during oxidation was observed at the vicinal NiAl(16,14,1) surface.[27] In that study, an increase in area of the energetically favored (110) facet has been observed upon oxidation. Here, a reformation of the stable (110) surface during oxidation is proven. Although the step edges may arrange in different orientations, in the following, we focus on step edges with an orientation parallel to the straight APDBs.

### C. Step edges imaged by AFM

Since the obtained signal of the AFM is the surface structure convoluted with the microscopic tip configuration, AFM images with atomic resolution directly at the step edges are very challenging without tailoring a monoatomic, extremely sharp and stiff tip. This is especially true for a structure with such closely spaced sites as in the aluminum oxide surface. Nevertheless, we were able to image the step edge in the oxide surface by AFM with unit-cell resolution on both terraces (Fig. 4). A lateral displacement of approximately 0.3 nm exists between the unit-cell lattices on both terraces. If one also considers the change of the height at the step edge

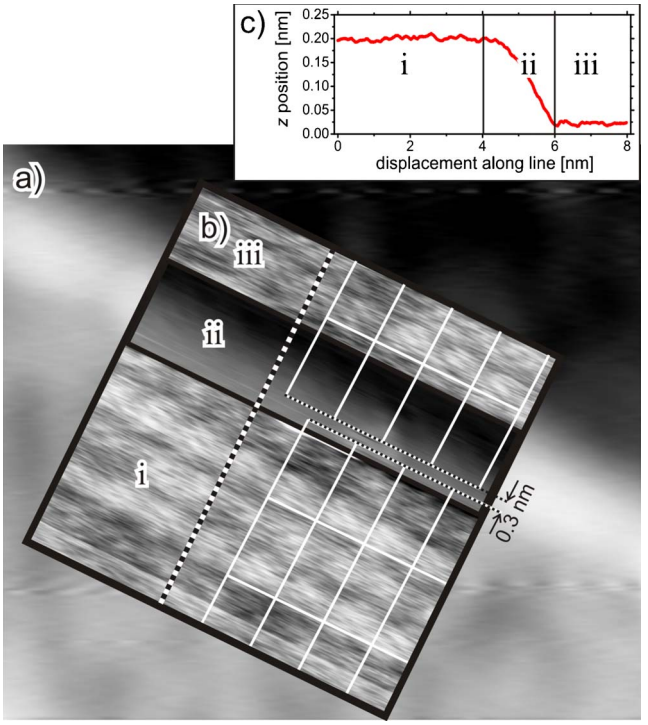


FIG. 4. (Color online) Picture of a step edge. a) STM picture, $12\times13$ nm$^2$, $U_{bias}=3$ V, and $I=100$ pA. b) AFM image of the step edge at the position shown in a), which is leveled to the upper terrace (i), the lower terrace (iii) and to the step edge (ii). The lattices of the surface unit cells on both terraces are pictured. A small gap between both lattices of 0.3 nm exists. The size of the image is $8\times8$ nm$^2$. The frequency shift was −2.2 Hz at a bias voltage of −150 mV. c) The $z$ displacement of the tip along the dotted line in b).

(0.2 nm) and one assumes that this is compensated at a lateral distance of 0.3 nm, the actual extension of the unit cell at the step edges is approximately 0.36 nm. The unit cell at a straight APDB is extended by approximately 0.3 nm,[26] which perfectly matches the value determined at the step edges. This means the stress, which accumulates due to a small lattice mismatch with the NiAl along the [1 −1 0] direction, can be relaxed at the step edges, not only at the APDB on a flat surface.

### D. Electronic structure

When the oxide film is imaged by STM with different bias voltages, the APDB appears in different heights (Fig. 5). In addition to this, the contrast of the step edges changes in a similar way. In Fig. 5(b), corresponding line profiles of the $z$ displacement are shown for different bias voltages. At certain voltages, e.g., −0.5 and +1.5 V, the APDBs are hardly visible and the step edges resemble simple steps of the $z$ position. At for instance +2 and +3 V, however, the APDBs appear as protrusions in the $z$ displacement. At these voltages, the step edges are also pictured as risings and not just as simple steps. It has to be noted that this effect is independent on the scan direction, i.e., forward or backward scan, and is therefore no artifact.

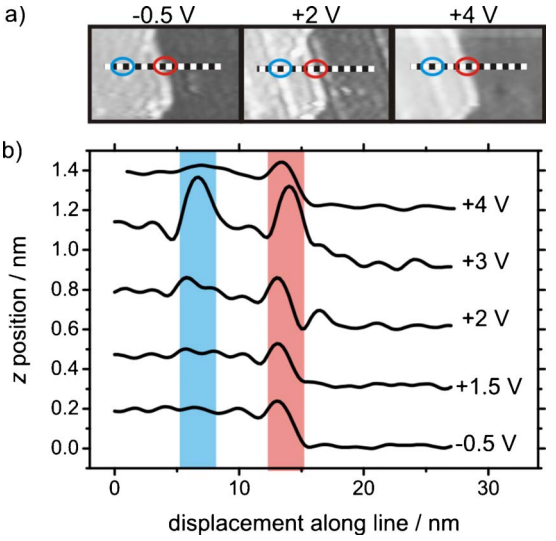


FIG. 5. (Color online) a) STM picture of the thin film aluminum oxide on NiAl(110) recorded with three different bias voltages (−0.5, +2, and +4 V). The size is $12\times20$ nm$^2$ and the tunneling current is 100 pA. The step edge between two terraces is marked by a red circle, the APDB by a blue circle. b) Profiles of the $z$ position recorded at the dotted line in figure a) at 5 different bias voltages (−0.5–+4 V). The position of the APDB is marked blue, the step edge red. At bias voltages where the APDBs are clearly visible as rising in the STM picture (i.e., at +2 V) there is also an additional rising at the step edge. Where the APDBs are hardly visible (i.e., at −0.5 V), the step edges appears as simple steps. For a better visibility, the profiles are shifted vertically.

STS shows that step edges and APDBs have very similar spectra while the spectrum of the domain is significantly different (Fig. 6). This means that step edges and APDBs have similar electronic structures, which are different from the domain. This explains why the APDBs and the step edges are imaged by STM in a similar way and the contrast changes with the bias voltage.

It follows from the peaks at energies between +2 and +3 eV that there exist unoccupied states at step edges and

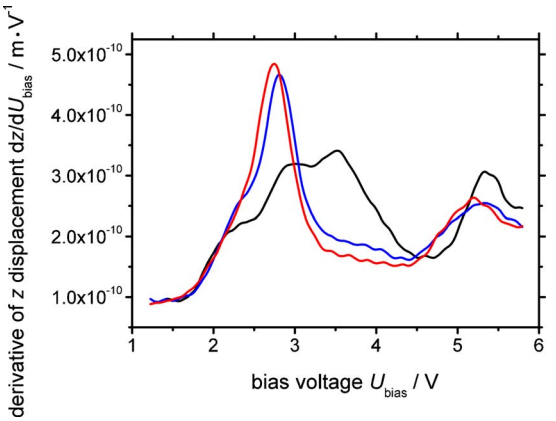


FIG. 6. (Color online) STS of domain (black line), APDB (blue) and step edge (red). The $z$ displacement differentiated with respect to the bias voltage as a function of the bias voltage shows similar spectra at the APDB and at the step edges while the spectrum at the domain is significantly different.

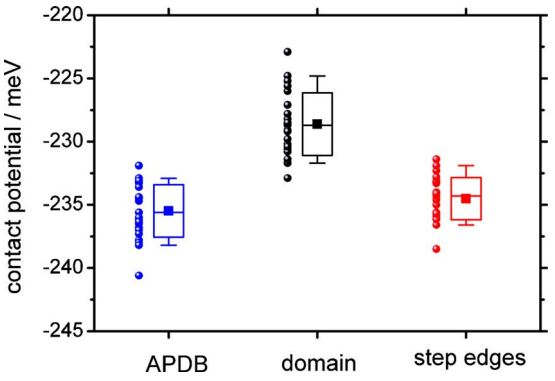


FIG. 7. (Color online) Contact potential spectroscopy. The determined contact potential at the domain (black), APDB (blue) and step edge (red) as well as the box plots of the statistical data are shown. The boxes indicate the range of the standard deviations and the whiskers the range of 5 to 95 % of the distribution. The small squares indicate the mean values. All measurements were performed with the same tip configuration at a frequency shift of −1.1 Hz. The minimum of the frequency shift with this tip configuration was −1.8 Hz.

APDBs at these energies. At the APDB, these unoccupied states in the aluminum oxide band gap are caused by oxygen deficiency and $F^{2+}$-like centers emerge.[10,24]

### E. Work function

Contact potentials were determined by Kelvin probe force microscopy at many sites on the domain, on APDBs and on step edges (Fig. 7). The recorded contact potential at APDBs and at step edges is approximately 5–10 meV smaller than at the domain. This means the work function at the APDBs and at the step edges is decreased. The real variations of the contact potential differences between domain and line defects are even larger, since the measured signal is the real contact potential difference convoluted with the tip geometry.[19,24,28] Furthermore, the determined contact potential difference depends also on the tip-sample distance.[22] In general, a smaller distance increases the size of the interaction and the determined difference of the contact potential. However, if the distance becomes too small, the probability that the tip restructures increases due to the enormous electrostatic field. This happens often particularly at step edges. Therefore, the tip-sample distance was set to a moderate value which corresponds to about 50% of the minimum in the frequency shift-distance curve. The recorded contact potential difference changes with the geometrical and chemical identity of the tip. Therefore, the measurements have to be performed with the same microscopic tip configuration on step edges, APDBs and domain.

### F. Interpretation: The structure of the step edge

In the previous paragraphs, we have shown thin film aluminum oxide develops a specific electronic and topographic structure at the substrate step edges. From the orientation of the step edges before and after oxidation, a restructuring of the substrate during oxidation is concluded. This means a very dynamic interaction between the substrate and the surface during the film preparation is confirmed. It may be assumed that the substrate step edges restructure during the film crystallization at high temperature,[12] which is the second step during film preparation. Due to the increase of the total length of the individual step edges which accompanies the restructuring, it might be that step edges are not energetically unfavorable. This might be connected with the extension of the unit cell at the step edges, which enables a strain release.

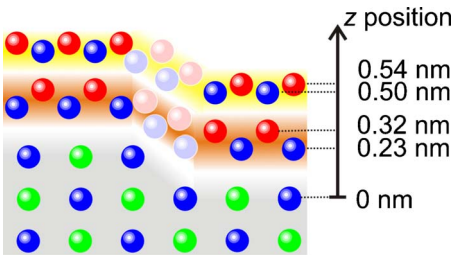


FIG. 8. (Color online) Simplified sketch of thin film aluminum oxide on NiAl(110) with one step edge of the substrate. Oxygen is plotted red, aluminum blue and nickel green. The oxide surface layer is marked with a yellow background, the oxide interface layer orange and the NiAl substrate gray. The $z$ values are taken from Ref. 3. The step height is 0.20 nm (Ref. 25).

The recorded work function decreases at the step edges in the same way as at the APDBs, i.e., in the range of 5–10 meV. Since the work function of the clean substrate surface is approximately 0.5 eV larger,[5] an uncovered metal atom would increase the determined work function dramatically. A different thickness of the oxide film, for instance only one aluminum and oxygen layer or even three aluminum and oxygen layers, can also be excluded, since this results in a dramatic variation of the work function.[22,29] Therefore, we conclude the substrate surface is fully covered by the two-layers-thick oxide film, even at the step edges, i.e., the film covers the substrate like a carpet. In Fig. 8, a simplified model of the step edges in thin film aluminum oxide on NiAl(110) is shown, where the two-layer-thick oxide film fully covers the substrate.

In addition to the comparable work function, the electronic structure of the APDBs and the step edges are very similar. Furthermore, the surface unit cells at both dislocations are extended by 0.3 nm. This means the characteristic features of the APDBs can also be found at the step edges. Consequently, we believe that the structure of the aluminum oxide at the substrate step edges has some similarities with the structure at the APDBs. An oxygen deficiency as in the APDBs is assumed in the step edges. A similar stoichiometry as in the APDB might be assumed, where it was determined to be $(NiAl)^{2-}_{substrate}(Al_{19}O_{28}Al_{28}O_{32})^{2+}$. Furthermore, it is concluded from the very similar bias spectra and from the same local work functions that $F^{2+}$-like centers evolve at the step edges, like in the APDBs. The $F^{2+}$-like centers, which are charged defect sites, significantly influence the chemical activity of the oxide surface. They are especially relevant for reactions with electron transfer, such as redox reactions. So, the higher reactivity which was assigned to the APDBs can also be concluded for the step edges.

The detailed study above is focused on step edges parallel to the straight APDBs (type I). In the STM, all step edges appear very similar and seem to have similar electronic structures [see Figs. 2 and 5(a)]. It might therefore be supposed that all step edges have properties similar to the step edges parallel to straight APDBs. This means a closed oxide film at the step edges with $F^{2+}$-like color centers seems to be a general feature. The orientations of the film on both terraces are identical at most step edges and similarities to APDBs of type I or II might therefore be concluded. At step edges separating domains of opposite reflection symmetry (A or B), similarities to the structure of reflection domain boundaries[30,31] may be assumed. In contrast to APDBs, which are caused by strain relief, reflection domain boundaries are created by linking two different domains during the film growth. Due to the possibility of additional translational displacement at reflection boundaries, a larger variety of structures has to be anticipated. A closed oxide film was proven at reflection domain boundaries by STM.[30,31] Therefore a closed oxide at step edges separating different domains may be concluded.

## V. CONCLUSION

STM and AFM were used to investigate the film properties at substrate induced steps within the thin aluminum oxide film on NiAl(110). A preferred orientation of the step edges along certain angles and a reorientation of the substrate step edges during oxidation have been found. The surface unit cell at the step edge is enlarged by approximately 0.3 nm, which is exactly the same value by which the surface unit cell at the APDB is extended. Using STS and Kelvin probe force spectroscopy, it was shown that the local electronic structure and the local work function at the step edges are very similar to those found at APDBs. A similar structure, i.e., an oxygen deficiency with $F^{2+}$-like centers, is therefore concluded for the step edges. Detailed investigation based on density functional theory may unveil further details of the oxide film at step edges.

## ACKNOWLEDGMENT

We cordially thank Gero Thielsch and Hans-Peter Rust for the technical support and many stimulating discussions.

*FAX: +49-30-8413-4105; heyde@fhi-berlin.mpg.de

[1] G. Ertl, H. Knözinger, F. Schüth, and J. Weitkamp, *Handbook of Heterogeneous Catalysis* (Wiley-VCH, New York, 2008).
[2] R. M. Jaeger, H. Kuhlenbeck, H. J. Freund, M. Wuttig, W. Hoffmann, R. Franchy, and H. Ibach, Surf. Sci. **259**, 235 (1991).
[3] G. Kresse, M. Schmid, E. Napetschnig, M. Shishkin, L. Kohler, and P. Varga, Science **308**, 1440 (2005).
[4] G. H. Simon, T. König, M. Nilius, H. P. Rust, M. Heyde, and H. J. Freund, Phys. Rev. B **78**, 113401 (2008).
[5] W. J. Song and M. Yoshitake, Appl. Surf. Sci. **251**, 14 (2005).
[6] T. Bertrams, A. Brodde, and H. Neddermeyer, J. Vac. Sci. Technol. B **12**, 2122 (1994).
[7] S. Schauermann, V. Johanek, M. Laurin, J. Libuda, and H. J. Freund, Chem. Phys. Lett. **381**, 298 (2003).
[8] M. Bäumer and H. J. Freund, Prog. Surf. Sci. **61**, 127 (1999).
[9] M. Kulawik, N. Nilius, H. P. Rust, and H. J. Freund, Phys. Rev. Lett. **91**, 256101 (2003).
[10] M. Schmid, M. Shishkin, G. Kresse, E. Napetschnig, P. Varga, M. Kulawik, N. Nilius, H. P. Rust, and H. J. Freund, Phys. Rev. Lett. **97**, 046101 (2006).
[11] C. L. Pang, H. Raza, S. A. Haycock, and G. Thornton, Phys. Rev. B **65**, 201401(R) (2002).
[12] K. F. McCarty, J. P. Pierce, and C. B. Carter, Appl. Phys. Lett. **88**, 141902 (2006).
[13] M. Heyde, G. H. Simon, H. P. Rust, and H. J. Freund, Appl. Phys. Lett. **89**, 263107 (2006).
[14] H. P. Rust, M. Heyde, and H. J. Freund, Rev. Sci. Instrum. **77**, 043710 (2006).
[15] W. Ho, J. Chem. Phys. **117**, 11033 (2002).
[16] M. Ziegler, N. Neel, A. Sperl, J. Kroger, and R. Berndt, Phys. Rev. B **80**, 125402 (2009).
[17] M. Nonnenmacher, M. P. Oboyle, and H. K. Wickramasinghe, Appl. Phys. Lett. **58**, 2921 (1991).
[18] C. Barth and C. R. Henry, Nanotechnology **17**, S155 (2006).
[19] H. O. Jacobs, P. Leuchtmann, O. J. Homan, and A. Stemmer, J. Appl. Phys. **84**, 1168 (1998).
[20] G. H. Enevoldsen, T. Glatzel, M. C. Christensen, J. V. Lauritsen, and F. Besenbacher, Phys. Rev. Lett. **100**, 236104 (2008).
[21] S. Kitamura, K. Suzuki, M. Iwatsuki, and C. B. Mooney, Appl. Surf. Sci. **157**, 222 (2000).
[22] T. König, G. H. Simon, H. P. Rust, and M. Heyde, J. Phys. Chem. C **113**, 11301 (2009).
[23] T. König, G. H. Simon, H. P. Rust, G. Pacchioni, M. Heyde, and H. J. Freund, J. Am. Chem. Soc. **131**, 17544 (2009).
[24] L. Heinke, L. Lichtenstein, G. H. Simon, T. König, M. Heyde, and H.-J. Freund, ChemPhysChem **110**, 2085 (2010).
[25] T. Kogita, M. Kohyama, and Y. Kido, Phys. Rev. B **80**, 235414 (2009).
[26] G. H. Simon, T. König, H. P. Rust, M. Heyde, and H. J. Freund, New J. Phys. **11**, 093009 (2009).
[27] S. Ulrich, N. Nilius, and H. J. Freund, Surf. Sci. **601**, 4603 (2007).
[28] U. Zerweck, C. Loppacher, T. Otto, S. Grafstrom, and L. M. Eng, Phys. Rev. B **71**, 125424 (2005).
[29] L. Giordano, F. Cinquini, and G. Pacchioni, Phys. Rev. B **73**, 045414 (2006).
[30] J. Libuda, F. Winkelmann, M. Baumer, H. J. Freund, T. Bertrams, H. Neddermeyer, and K. Muller, Surf. Sci. **318**, 61 (1994).
[31] K. Højrup Hansen, T. Worren, E. Lægsgaard, F. Besenbacher, and I. Stensgaard, Surf. Sci. **475**, 96 (2001).